# Modelling atmospheric and induced non-tidal oceanic loading contributions to surface gravity and tilt measurements

Jean-Paul Boy, Laurent Longuevergne, Frédéric Boudin, Thomas Jacob, Florent Lyard, Muriel Llubes, Nicolas Florsch, Marie-France Esnoult

## HAL Id: hal-00708046
## https://hal.archives-ouvertes.fr/hal-00708046

# Modelling atmospheric and induced non-tidal oceanic loading contributions to surface gravity and tilt measurements

Jean-Paul Boy [1, 2], Laurent Longuevergne [3], Frédéric Boudin [4], Thomas Jacob [4], Florent Lyard [5], Muriel Llubes [5] and Nicolas Florsch [6]

(1)  EOST/IPGS (UMR 7516 CNRS-ULP), 5 rue René Descartes, 67084 Strasbourg, France

(2)  NASA GSFC, Planetary Geodynamics Laboratory, Code 698, Greenbelt, MD 20771, USA.

(3)  Bureau of Economic Geology, Jackson School of Geosciences, The University of Texas at Austin,  PO Box X, Austin, TX 78713, USA.

(4)  Géosciences Montpellier (UMR 5243), Université Montpellier 2, Place E. Bataillon, 34095 Montpellier, France

(5)  LEGOS (UMR5566), 14 avenue Edouard Belin, 31400 Toulouse, France.

(6)  UMMISCO/ IRD, UPMC/Paris  and Dpt of Mathematics and Applied Mathematics, Cape Town University (South Afriqca).

**Abstract**

We investigate the contribution of atmospheric and its induced non-tidal oceanic loading effects on surface time-varying gravity and tilt measurements for several stations in Western Europe. The ocean response to pressure forcing can be modelled accordingly to the inverted barometer assumption, i.e. assuming that air pressure variations are fully compensated by static sea height changes, or using ocean general circulation models. We validate two runs of the HUGO-m barotropic ocean model by comparing predicted sea surface height variations with a hundred of tide gauge measurements along the European coasts. We then show that global surface pressure field, as well as a barotropic high-resolution ocean model forced by air pressure and winds allow a significant and systematic reduction of the variance of gravity and tilt residuals.

We finally show that precise gravity measurements with superconducting gravimeters allow the observation of large storm surges, occurring in the North Sea, even for inland stations. However, we also show that the continental hydrology contribution cannot be

neglected. Thanks to their specific sensitivity feature, only tiltmeters closed to the coast can clearly detect the loading due to these storm surges.

**Keywords**

Atmospheric loading, non-tidal oceanic loading, superconducting gravimeters, hydrostatic tiltmeters, storm surges.

**1. Introduction**

Beside solid Earth tides, ocean tidal loading and hydrology at seasonal timescales, atmospheric and induced oceanic loading effects are one of the major sources of surface gravity and tilt variations, over a large frequency band (see, for example, Warburton and Goodkind, 1977; Dal Moro and Zadro, 1998; Boy *et al.*, 2002; Neumeyer et al., 2004; Boy *et al.*, 2006). Thanks to significant improvements of numerical weather modeling, classical empirical corrections, such as barometric admittance for gravity (Warburton and Goodkind, 1977) or tilts (Dal Moro and Zadro, 1998) can nowadays be replaced by physical models using global atmospheric datasets and Green's function formalism (see, for example, Boy *et al.*, 2002; Neumeyer et al., 2004).

A precise estimation of atmospheric loading effects requires a model of the ocean response to pressure forcing. As a first approximation, the inverted barometer (Wusch and Stammer, 1997) assumes that static sea surface height variations compensate air pressure changes. If this model is valid for long periods (typically larger than a month), this is not the case at higher frequencies; the dynamic of the oceans cannot be neglected. With the increased accuracies of radar altimeters (Topex/Poseidon, Jason, etc.) and space gravity missions (Gravity Recovery And Climate Experiment), this simple approximation has been replaced by dynamic barotropic (Hirose *et al.*, 2001; Carrère and Lyard, 2003) or baroclinic (Dobslaw and Thomas, 2005) ocean models, forced by air pressure and winds. Because of its higher spatial sampling, we choose to use the barotropic HUGO-m model (Carrère and Lyard, 2003), forced by 6-hourly (0.5 degree run) or 3-hourly (0.25

degree run) ECMWF (European Centre for Medium-range Weather Forecasts) air pressure and winds. Although its sea surface height outputs are provided on a regular grid, the model is run on a finite element grid with spatial resolution of a few kilometres along the coasts.

The aim of this paper is to show the improvement in terms of reduction of variance of gravity or tilt residuals, when correcting atmospheric and induced oceanic loading effects using global circulation models and Green's function formalism. In previous studies, Boy *et al.* (2002) and Boy and Lyard (2008) showed that better gravity corrections are achieved using global surface pressure field provided by meteorological centers, and using barotropic non-tidal ocean models forced by air pressure and winds.

Regarding surface gravity measurements, we used a higher resolution (0.25 degree and 3-hourly, instead of 0.5 degree and 6 hourly) of the HUGO-m model (Carrère and Lyard, 2003), including some semi-enclosed basins such as the Baltic Sea which were not present in the oldier version used in Boy and Lyard (2008). In this paper, we also investigate the impact in terms of reduction of tilt variance, when correcting from atmospheric and non-tidal induced oceanic effects, using the same models and the same formalism.

Although Fratepietro et al. (2006) and Boy and Lyard (2008) have already showed comparisons between storm surge loading and superconducting gravity records, we also investigate the loading contribution of the large November 2007 storm surge in the North Sea, on surface gravity and tilt measurements in Western Europe. As surges are usually characterized by heavy rainfall, we also compute hydrological loading effects, using the GLDAS/Noah (Global Land Data Assimilation System) (Rodell *et al.*, 2004).

**2. Computation of loading effects**

In this paper, we are studying 8 European superconducting gravimeters (Vienna in Austria, Membach in Belgium, Strasbourg in France, Metsähovi in Finland, Bad Homburg, Moxa and Wettzell in Germany and Medicina in Italy), as well as 5 stations equipped with long baseline hydrostatic tiltmeters (Boudin *et al.*, 2008) (CERGA, Ploemeur, Sainte-Croix-aux-Mines, Infruts and Titou, all in France). Their locations are shown in Figure 1.

## 2.1. Green's functions

We compute the atmospheric and induced non-tidal ocean loading using the Green's function formalism (Farrell, 1972). Assuming a SNREI (Spherically Symmetric Non-Rotating, Elastic and Isotropic) Earth model, the Green's functions are only function of the angular distance $\psi$ between the load and where the loading is computed.

Classically, the gravity Green's function is decomposed into an elastic part (Equation 1) and the direct Newtonian attraction.

$$GE(\psi) = -\frac{G}{g_0} \sum_{n=1}^{\infty} \left(2h_n' - (n+1)k_n'\right) P_n(\cos\psi) \tag{1}$$

where $G$ and $g_0$ are respectively the universal constant of Gravitation and the mean surface gravity. $P_n(\cos\psi)$ is the Legendre polynomial of degree n; $h_n'$ and $k_n'$ are the load Love numbers, computed using PREM (Dziewonski and Anderson, 1981) model.

The Newtonian attraction is computed, using only surface pressure, yet considering its thickness, following Boy *et al.* (2002) and Merriam (1995). More precise estimation of Newtonian attraction, taking into account the complete 3-D structure of the atmosphere can be found in Neumeyer *et al.* (2004).

The tilt Green's function is equal to (Farrell, 1972):

$$T(\psi) = \frac{G}{g_0^2} \sum_{n=1}^{\infty} \left(1 + k_n' - h_n'\right) \frac{\partial P_n(\cos\psi)}{\partial \psi} \tag{2}$$

We assume that the atmosphere and the oceans act both as a thin layer loading process at the Earth's surface and only depend on the total surface pressure.

The Green's functions are then convolved with the total surface pressure, in order to compute the loading effects at the different sites. The total pressure is the sum of the air pressure and the pressure induced by the ocean response. In the case, of the classic inverted barometer assumption (Wunsch and Stammer, 1997), air pressure changes are compensated by static sea surface height.

In addition, we estimate the contribution for the continental hydrology (soil-moisture, snow and to a smaller extend canopy water) using the GLDAS/Noah (Global Land Data Assimilation System) (Rodell *et al.*, 2004) model, using the same formalism.

## 2.2. Comparison of HUGO-m and the IB assumption with tide gauges observation along the European coast.

One of the goals of this paper is to show the improvement in terms of reduction of the variance of residuals using a barotropic ocean model, compared to the classical inverted barometer assumption. Because of its temporal (6- or 3-hourly) and spatial (0.5 or 0.25 degree), we choose to use two versions of the HUGO-m models (Carrère and Lyard, 2003). Boy and Lyard (2008) already showed that the "low" resolution model allows a systematic and significant reduction of superconducting gravimeter residuals for periods between typically 2 and 100 days. In this paper, we want to investigate how residuals are reduced with the higher resolution version of HUGO-m.

As we are focusing on instruments installed in Western Europe, we first want to validate these two barotropic ocean models with about 100 tide gauge records, along the European coasts (see Figure 1).
Table 1 gives the mean RMS of the de-tided tide gauge residuals, after correcting for the high-frequency ocean response, i.e. the inverted barometer assumption and both HUGO-m models. The barotropic ocean models, forced by air pressure and winds better explain the observed sea surface height variations, compared to the IB assumption. As expected,

the improvement occurs for periods smaller than typically a month. Because of its higher temporal and spatial sampling, the high resolution HUGO-m model (3-hourly and 0.25°) shows a higher correlation with the de-tided tide gauges.


## 3. Reduction of the variance of gravity and tilt residuals

### 3.1. Superconducting gravimeters

The processing of the superconducting gravimeter data is the same as the one adopted by Boy and Lyard (2008). Minute raw gravity and pressure data are first corrected for major perturbations (Crossley *et al.*, 1993) and then filtered to hourly samples. Gravity are then corrected from polar motion and length-of-day induced effects (Wahr 1985), using EOPC04 series from the International Earth Rotation Service (IERS), assuming an elastic Earth and an equilibrium pole tide, including self-attraction and loading terms (Agnew & Farrell 1978). Long period tides (solid Earth and ocean tidal loading) are removed using Dehant *et al.* (1999) theoretical gravimetric factors and NAO99b ocean tide model (Matsumoto *et al.* 2000). Finally, tidal analyses are performed using the ETERNA package (Wenzel, 1997), using the different atmospheric loading corrections

Table 2 gives the RMS (root mean square) of the gravity residuals, for the ECMWF/IB, ECMWF/HUGO-m low resolution and ECMWF/HUGO-m high resolution atmospheric and induced oceanic loading corrections. Except for the long time series for Wettzell, which is affected by a strong seasonal signal, the variance of the residuals are smaller when using the HUGO-m models, compared to the classical inverted barometer approximation. These results are in agreement with the previous study by Boy and Lyard (2008). The reduction of the RMS of gravity residuals is larger using the high resolution HUGO-m model, than using the lower resolution run, except for Strasbourg and Medicina. As the Baltic Sea is only taken into account in the high resolution model, the reduction of variance is much larger for Metsähovi. Figure 2 shows the amplitude of the gravity residuals with the different models of oceanic response to pressure forcing, for

Membach (Belgium) station. The barotropic ocean models allow a significant and systematic reduction of the gravity residuals, for periods between typically between 1 day and a few months, compared to the inverted barometer assumption. Although the differences between IB and a dynamic ocean response to pressure forcing increase with the frequency, there is no significant reduction of the gravity residuals for sub-daily periods. We have to further investigate the validity of other corrections applied to gravity observations. One possible improvement should be the use of regional 3-D atmospheric model, instead of global pressure field.

## 3.2. Long-base hydrostatic tiltmeters

Atmospheric pressure variations induce tilt variations according two major deformation processes: surface loading, described here by the Green function formalism and site effects. These effects are due to topography or local variation of the mechanical properties of the rocks and locally modify the regional stress field (e.g. Harrison, 1976). Saint-Venant's principle states the modification of the stress field has a characteristic length that is close to the size of the heterogeneities. This means that long-base tiltmeters are less sensitive to these local effects.

We process tiltmeter data in a similar way than for gravity, except that all tides (including the long period constituents) are removed by least-square fitting by ETERNA. We have not included in our loading computations the contribution of the ocean pole tide. We choose to model the non-tidal oceanic loading using the high resolution HUGO-m model, as this model is in better agreement with tide-gauge observations, and to a smaller extent to surface gravity observations.

We performed tidal analyses of the 10 tilt records (2 components per station), with different global atmospheric, oceanic and hydrological corrections:

1. no correction,
2. ECMWF assuming IB,
3. ECMWF and HUGO-m,

4. ECMWF, IB and GLDAS,

5. ECMWF, HUGO-m and GLDAS.

The duration of each station varies from about 1 year for CERGA and Infuts, to about 2 years for Titou and Ploemeur, and almost 3 years for Ste Croix-aux-Mines. Table 3 gives the RMS of the residuals after tidal analysis with the different loading correction.

Some of the tiltmeter records are affected by strong long period variations which may be caused by instrumental drift, but also by local effects. In fact, all these stations have been installed to study local or regional hydrology contributions (e.g. Longuevergne et al. 2008). The station with the lowest noise level is Sainte-Croix-aux-Mines, where the about 100-m hydrostatic tiltmeters have been installed deeply in an old mine.

Table 3 gives the RMS of the tilt residuals, after tidal analyses with the different atmospheric (ECMWF 3-hourly), oceanic (inverted barometer or HUGO-m 3-hourly) and hydrological (GLDAS 3-hourly) loading corrections. Except for the following components N005 of CERGA, N111 for Infruts and N094 for Titou, the tilt residuals are smaller when modelling the atmospheric and the induced non-tidal oceanic loading contributions. In most of case, the residuals are smaller using HUGO-m barotropic ocean model than the inverted barometer assumption. However, compared to gravity observations with superconducting gravimeters, tiltmeter measurements are characterized by high noise levels. An improvement of the atmospheric loading correction for mountainous stations (like Cerga, Infruts or Titou) would require the use of finite-element modelling taking into account the surrounding topography (see Kroner et al., 2005).

Figure 3 shows the spectrum of tilt residuals for Sainte Croix-aux-Mines instruments, respectively with no loading correction, ECMWF-IB and ECMWF-HUGO-m. The estimation of loading effects due to the atmosphere and the oceans using general circulation models allow a significant reduction of the residuals, for periods typically

between 1 day and about 2 months, i.e. in the same frequency domain than for surface gravity observations.


## 4. Contribution of storm surges to gravity and tilt variations

Fratepietro et al. (2006) and Boy and Lyard (2008) already computed the non-tidal oceanic loading effects on surface gravity measurements due to storm surges over the North-Western European shelf, and the comparison with superconducting gravimeters. In this section, we show the differences between both HUGO-m barotropic models: the "low resolution" (0.5 degree, 6-hourly) used in Boy and Lyard (2008) and the higher resolution (0.25 degree, 3-hourly). In particular, the new version includes the Baltic Sea, which has a significant contribution to gravity variations in Metsähovi (Virtanen and Mäkinen, 2003). We also extend our study to tiltmeter measurements, although only one instrument (Ploemeur) is located near the Atlantic Ocean coasts.

Compared to Boy and Lyard (2008), we choose a larger and more recent storm surge, which occurred in November 2007. Figure 4 shows the comparison between sea surface height variations measured by 8 tide gauge stations along the North Sea coasts and modelled by the low and high resolution HUGO-m runs. Only the latest (0.25 degree and 3-hourly) model is able to match the high amplitudes (more than 2 meters in Dunkerque and Cuxhaven) reached the 9th of November 2007.

Figure 5 shows the comparison between gravity residuals (after correction of tidal, polar motion and atmospheric contributions), the two non-tidal oceanic loading models and the continental hydrology loading effects modelled with GLDAS/Noah.
As we are not taking into account the topography around each station, the hydrology loading estimates are not very accurate for Moxa. However, Figure 5 also shows the significant contribution of soil-moisture variations, compared to the non-tidal ocean loading effects in a case of a storm surge for gravity variations.

As only the high resolution model includes the Baltic Sea, the correlation between non-tidal oceanic loading and gravity residuals are larger than with the low resolution.

Figure 6 shows the tilt residuals without any loading correction in Sainte-Croix-aux-Mines in November 2007. The atmospheric (ECMWF 3-hourly) and non-tidal oceanic (HUGO-m 3-hourly), as well as the hydrological loading (GLDAS) are also plotted. The loading contribution of the storm surge can be seen in the N120 component, as in a smaller extent in the N37, although the correlation is not as large as for gravity measurements in Strasbourg. We could not observe the storm surge induced tilt changes in any other tiltmeters, because their noise levels are much larger.

As tilt measurements are mostly sensitive to regional hydrology, the loading modelled with GLDAS soil-moisture and snow does not have a strong impact, at least for this storm surge. In order to have a better estimate of hydrological contributions, a regional model would be required (Longuevergne et al., 2008).

## 5. Discussion and Conclusion

As it has already been shown in a previous study by Boy and Lyard (2008), HUGO-m barotropic ocean model allows a significant and systematic reduction of gravity residuals, compared to the classical inverted barometer approximation, for periods between a few days and 100 days. The higher resolution (3 hourly and 0.25 degree) model shows some improvement compared to the lower resolution version (6 hourly and 0.5 degree), for stations in the vicinity of the coasts (for example, Membach), or near semi-enclosed basins that were not taken into account (for example, Metsähovi). However, there is still no improvement for sub-daily periods, even with the model forced by 3-hourly ECWMF winds and pressure. The reduction of surface gravity variations in this frequency domain may require more precise atmospheric loading computations, using high resolution (both temporally and spatially) regional 3-D atmospheric models. There are indeed variations of vertical profiles of temperature, and therefore air density at daily and sub-daily periods.

Although tilt measurements can be affected by local effects, such as cavity, the use of global atmospheric and oceanic models allows a reduction of the residuals, within about the same frequency band that for surface gravity variations. However, there are still large un-modelled atmospheric and hydrological contributions using the Green's function formalism and global fields. An improvement of our atmospheric loading estimations would require using finite-element modelling to account for the topography surrounding of each stations (Kroner *et al.*, 2005). The modelled local effects are generally described as linear function of local pressure measurements. However, in Sainte-Croix-aux-Mines, residuals are no more correlated with pressure variations, indicating that this 100-m long base tiltmeter is not sensitive to site effects.

Because of its higher temporal and spatial sampling, the high resolution HUGO-m allows a better modelling of storm surges in the North Sea, both in terms of sea surface height variations (as seen with the comparison with tide gauges) and induced gravity variations. As shown by Boy and Lyard (2008), the hydrological contribution cannot be neglected. However, because of the small wavelength and short period characteristics of storm surge related rainfall events, loading estimates should not only include global continental hydrology models, but also local modelling (Meurers *et al.*, 2007; Van Camp *et al.*, 2006).

Except for tiltmeters located near the coasts, it the observation of storm surge induced tilt changes seems quite difficult. Indeed, these instruments have a higher noise level due to local environmental conditions, as well to different sensitivities. We were able to detect the November 2007 storm surge in Sainte-Croix-aux-Mines, because its amplitude was large (about 2 meters of sea surface height increase), and also because the two instruments are characterized by an extremely low noise level (RMS of a few mas).

**Acknowledgement**

## References

Agnew, D. C. and Farrell, W. E., 1978. Self-consistent equilibrium ocean tides, *Geophys. J. R. astr. Soc.*, **55**, 171-181.

Boudin, F., Bernard, P., Longuevergne, L., Florsch, N., Larmat, G., Courteille, C., Blum, P.-A., Vincent, T. and Kammentaler, M., 2008. A silica long base tiltmeter with high stability and resolution, *Rev Sci Instrum.*, **79** (3), 034502.

Boy, J.-P., and Lyard, F., 2008. High-frequency non-tidal ocean loading effects on surface gravity measurements, *Geophys. J. Int.*, **175**, 35–45.

Boy, J.-P., Ray, R. and Hinderer, J., 2006. Diurnal atmospheric tide and induced gravity variations, *J. Geodynamics.*, **41**, 253-258.

Boy, J.-P., Gégout, P. and Hinderer, J., 2002. Reduction of surface gravity data from global atmospheric pressure loading, *Geophys. J. Int.*, 149, 534-545.

Carrère, C. and Lyard, F., 2003. Modeling the barotropic response of the global ocean to atmospheric wind and pressure forcing - Comparisons with observations, *Geophys. Res. Lett.*, **30** (6), 1275, doi:10.1029/2002GL016473.

Crossley, D. J., Hinderer, J., Casula, G., Francis, O., Hsu, H.-T., Imanishi, Y., Meurers, B., Neumeyer, J., Richter, B., Shibuya, K., Sato, T., and van Dam, T., 1999. Network of superconducting gravimeters benefits several disciplines, EOS, **80**, 121-126.

Crossley, D. J., Hinderer, J., Jensen, O. and Xu, H., 1993. A slewrate detection criterion applied to SG data processing, *Bull. d' Inf. Mar´ees Terr.,* **117,** 8675–8704.

Dal Moro, G. and Zadro, M., 1998. Subsurface deformations induced by rainfall and atmospheric pressure: tilt/strain measurements in the NE-Italy seismic area, *Earth Planet. Sci. Let.*, **164**, 193-203.

Dehant, V., Defraigne, P. and Wahr, J., 1999. Tides for a convective Earth, *J. geophys. Res.,* **104** (B1), 1035–1058

Dobslaw, H. and Thomas, M., 2005. Atmospheric induced oceanic tides from ECMWF forecasts, *Geophys. Res. Lett.,* **32,** L10615, doi:10.1029/2005GL022990.

Dziewonski, A.M. and Anderson, D.L., 1981. Preliminary Reference Earth Model, *Phys. Earth planet. Inter.,* **25,** 297–356.

Farrell, W. E., 1972. Deformation of the Earth by surface loads, *Rev. Geophys. Space Physics*, **10**, 761-797.

Fratepietro, F., Baker, T. F., Williams, S. D. P. and Van Camp, M., 2006. Ocean loading deformations caused by storm surges on the northwest European shelf, *Geophys. Res. Lett.*}, **33**, L06317, doi:10.1029/2005GL025475.

Harrison, J., 1976. Cavity and topographic effect in tilt and strain measurement, *J. Geophys. Res.*, **81** (2), 319–328.

Hirose, N., Fukumori, I., Zlotnicki, V. and Ponte, R.M., 2001. Modeling the high-frequency barotropic response of the ocean to atmospheric disturbances: sensitivity to forcing, topography and friction, *J. geophys. Res.,***106** (C12), 30 987–30 995.

Kroner, C., Jahr, T., Kuhlmann, S. and Fisher, K. D., 2005. Pressure-induced noise on horizontal seismometer and strainmeter records evaluated by finite element modeling, *Geophys. J. Int.*, **161** (1), 167-178.

Longuevergne, L., Florsch, N., Boudin, F., Oudin, L. and Camerlynck, C. 2008. Coupled mechanical and hydrological modeling of the deformation induced by natural hydrologically active fractures, *Geophys. J. Int.*, accepted.

Matsumoto, K., Takanezawa, T. and Ooe, M., 2000. Ocean Tide Models Developed byAssimilating TOPEX/POSEIDON Altimeter Data into Hydrodynamical Model: a Global Model and a Regional Model Around Japan, *J. Oceanogr.,* **56,** 567–581.

Merriam, J. B., 1992. Atmospheric pressure and gravity, *Geophys. J. Inter.*, 109, 488-500.

Neumeyer, J., Hagedoorn, J., Leitloff, J. and Schmidt, T., 2004. Gravity reduction with three-dimensional atmospheric pressure data for precise ground gravity measurements, *J. Geodynamics*, **38** (3-5), 437-450.

Meurers, B., Van Camp, M. and Petermans, T., 2007. Correcting superconducting gravity time-series using rainfall modelling at the Vienna and Membach station and application to Earth tide analysis, *J. Geodesy*, **81** (11), 703–712.

Rodell, M., Houser, P. R., Jambor, J., Gottschalck, J., Mitchell, K., Meng, C.-J., Arsenault, K., Cosgrove, B., Radakovich, J., Bosilovich, M., Entin, J. K., Walker, J. P., Lohmann, D. and Toll, D., 2004. The Global Land Data Assimilation System, *Bull. Amer. Meteor. Soc.*, **85** (3), 381-394.

Van Camp, M., Vanclooster, M., Crommen, O., Petermans, T., Verbeeck, K., Meurers, B., van Dam., T. and Dassargues, A., 2006. Hydrogeological investigations at the Membach station, Belgium, and application to correct long periodic gravity variations, *J. Geophys. Res.*, **111**, B10403, doi: 10.1029/2006JB004405.

Virtanen, H. and Mäkinen, J., 2003. The effect of the Baltic Sea level on gravity at the Metsähovi station, *J. Geodynamics*, **35**, 553-565.

Wahr, J. M., 1985. Deformation induced by polar motion, *J. Geophys. Res.*, **90** (B11), 9363-9368.

Warburton, R. J. and Goodkind, J. M., 1977. The influence of barometric pressure variations on gravity, *Geophys. J. R. astr. Soc.*, **48** (3), 281-292.

Wenzel H. G., 1997. The nanogal software: Earth tide data processing package ETERNA 3.30, *Bull. d'Inf. Marées Terr.*, 124, 9425-9439.

Wunsch, C. and Stammer, D., 1997. Atmospheric loading and the oceanic inverted barometer effect, *Rev. Geophys.*, **35**, 79-107.
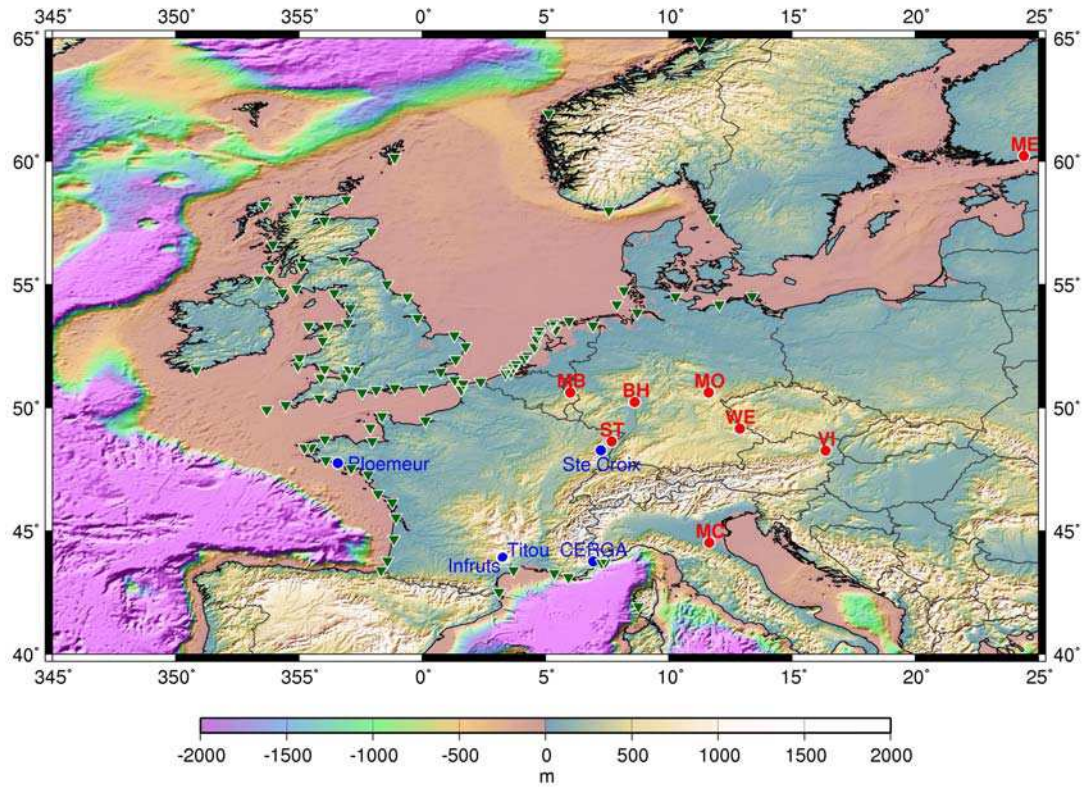
Figure 1: Map of superconducting gravimeters (red circles), and tide gauges (green triangle) in Europe and hydrostatic tiltmeters (blue circles) in France.
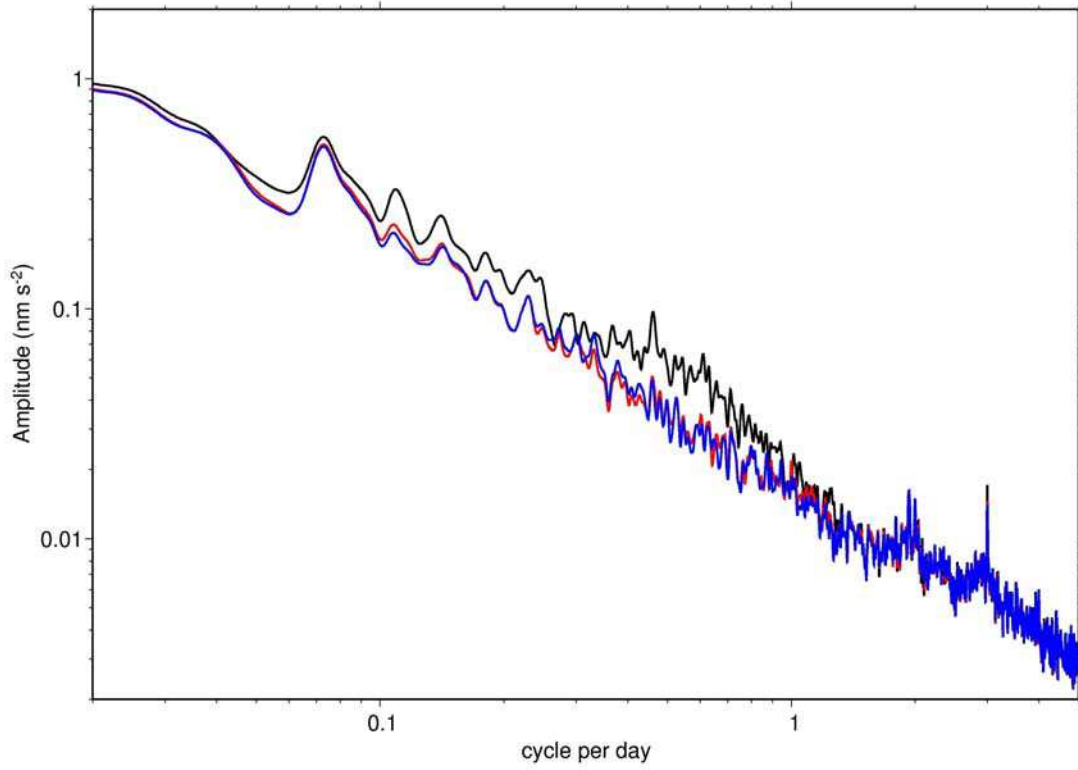
Figure 2: Amplitude (IB, HUGO-m low and high resolutions are respectively in black, red and blue) of gravity residuals after tidal analysis for Membach instrument.
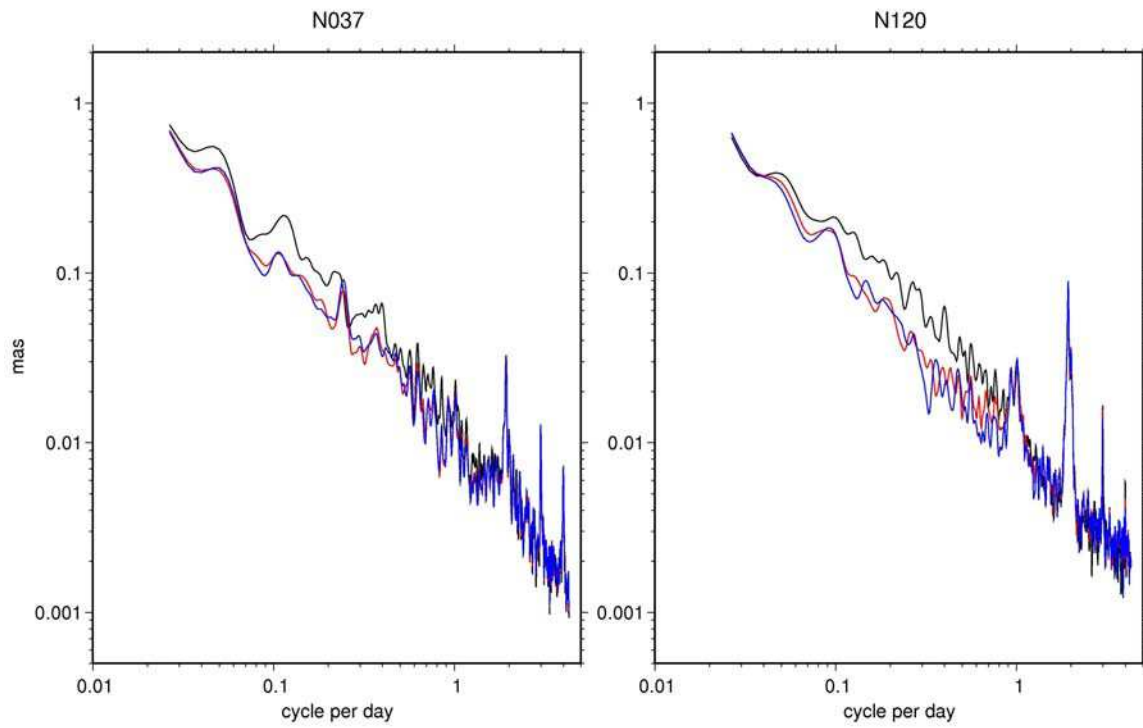
Figure 3: Amplitude of tilt residuals after tidal analysis of Sainte Croix-aux-Mines instruments, with no loading correction, ECMWF-IB, and ECMWF-HUGO-m correction respectively in black, red and blue.
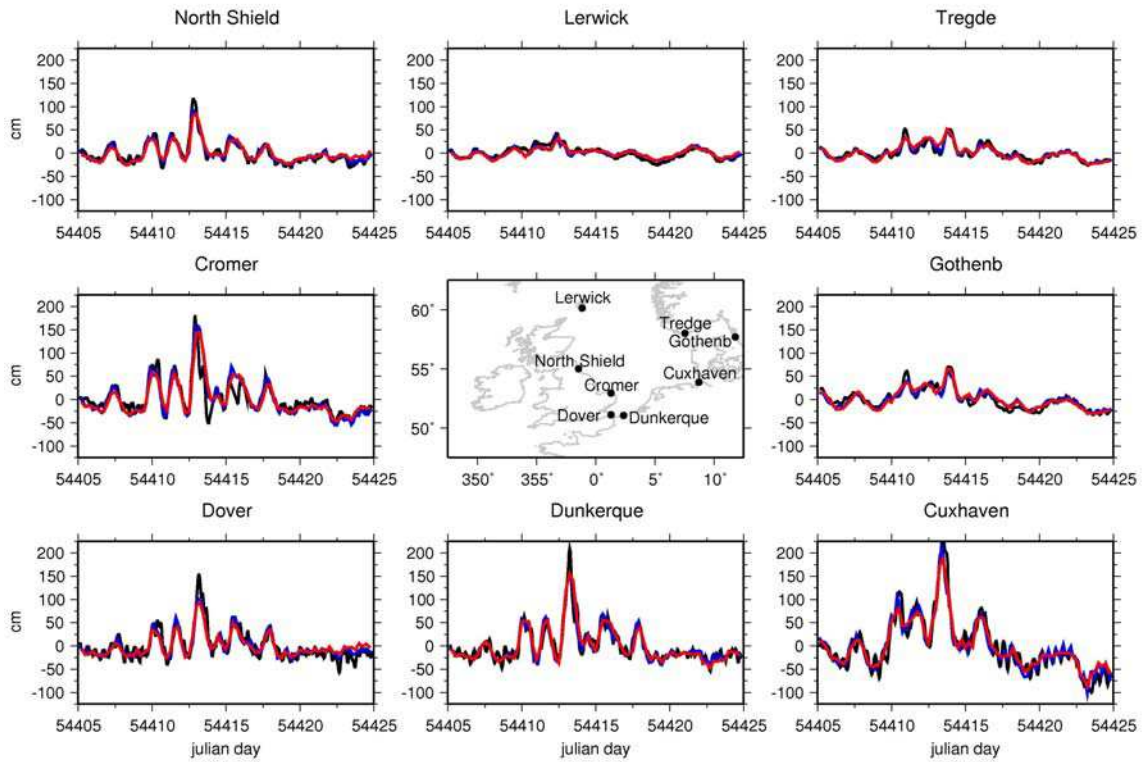
Figure 4: Comparison of de-tided tide gauge measurements (black) and sea surface height variations from HUGO-m low (red) and high (blue) resolution models, for the November 2007 storm surge.
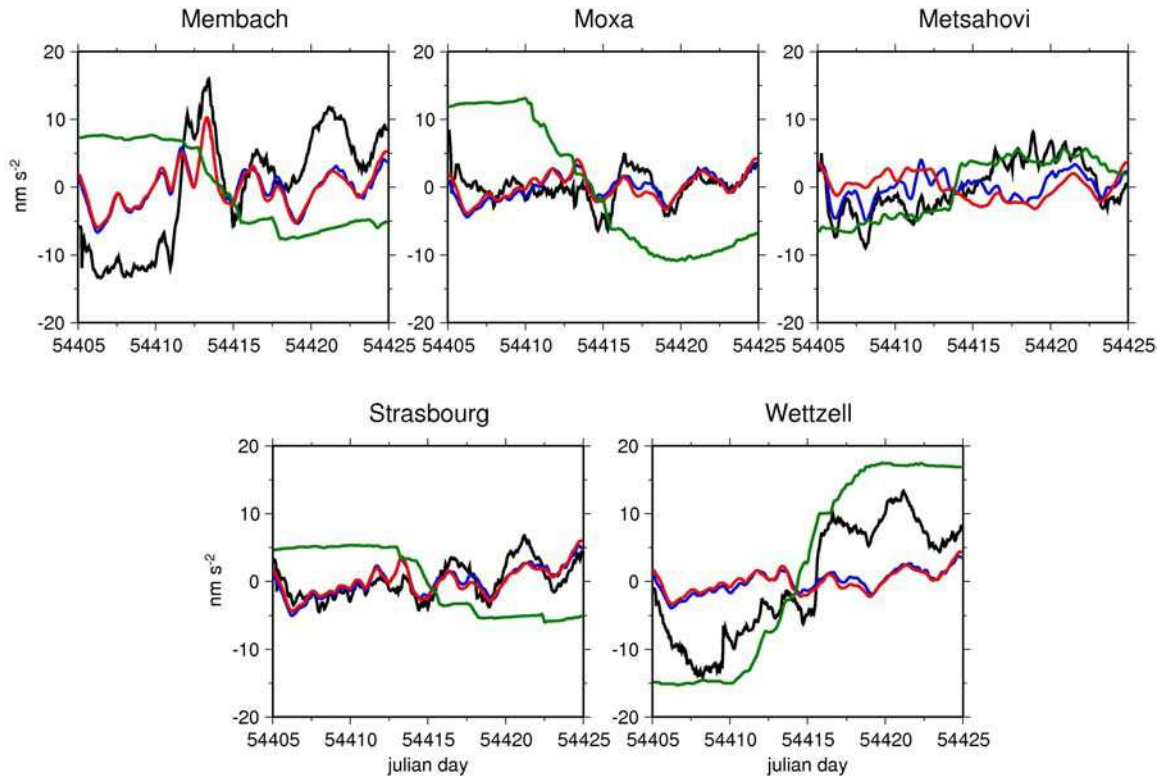
Figure 5: Gravity residuals (black), non-tidal oceanic loading (the low and high resolution models are respectively in red and blue) and continental hydrology loading (green).
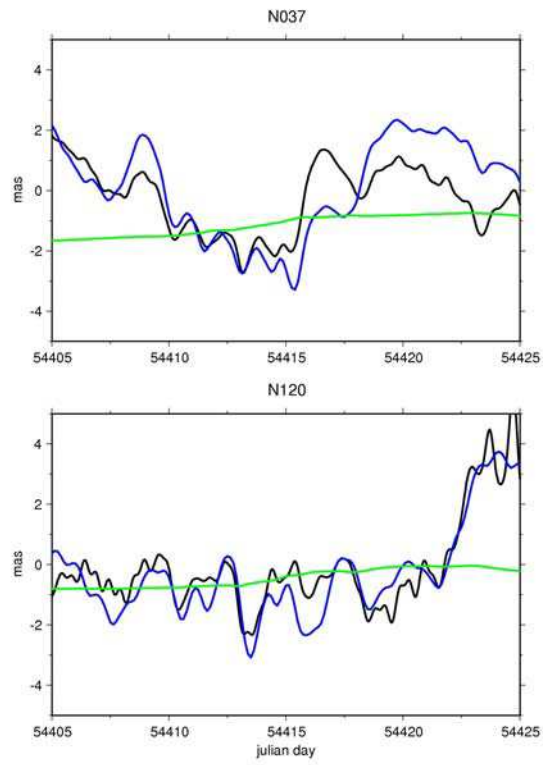
Figure 6: Tilt residuals in Sainte-Croix-aux-Mines (black), atmospheric and non-tidal oceanic loading (blue) and continental hydrology loading (green).

| No correction | Inverted barometer | HUGO-m (6-hourly, 0.5°) | HUGO-m (3-hourly, 0.25°) |
|---|---|---|---|
| 22.95 cm | 20.83 cm | 16.95 cm | 15.94 cm |

Table 1: Amplitude of de-tided tide gauge residuals, after correcting for the inverted barometer assumption, or the HUGO-m models.

| | ECMWF-IB | ECMWF/HUGO-m (low resolution) | ECMWF/HUGO-m (high resolution) |
|---|---|---|---|
| BH (2002/01-2007/04) | 16.757 nm s$^{-2}$ | 16.319 nm s$^{-2}$ | 16.333 nm s$^{-2}$ |
| MB (2002/01-2008/03) | 13.997 nm s$^{-2}$ | 13.789 nm s$^{-2}$ | 13.736 nm s$^{-2}$ |
| MC (2002/01-2007/08) | 16.697 nm s$^{-2}$ | 16.066 nm s$^{-2}$ | 16.080 nm s$^{-2}$ |
| ME (2003/11-2008/03) | 15.562 nm s$^{-2}$ | 15.200 nm s$^{-2}$ | 14.476 nm s$^{-2}$ |
| MO (2002/01-2008/03) | 11.909 nm s$^{-2}$ | 11.741 nm s$^{-2}$ | 11.608 nm s$^{-2}$ |
| ST (2002/01-2008/04) | 14.006 nm s$^{-2}$ | 13.896 nm s$^{-2}$ | 13.921 nm s$^{-2}$ |
| VI (2002/01-2006/12) | 7.966 nm s$^{-2}$ | 7.467 nm s$^{-2}$ | 7.407 nm s$^{-2}$ |
| WE (2002/01-2007/04) | 36.199 nm s$^{-2}$ | 36.285 nm s$^{-2}$ | 36.382 nm s$^{-2}$ |
| WE (2007/05-2007/12) | 6.943 nm s$^{-2}$ | 6.789 nm s$^{-2}$ | 6.672 nm s$^{-2}$ |

Table 2: RMS of gravity residuals, after tidal analysis with the different atmospheric and induced ocean loading corrections.

| | direction | No corr. | ECMWF IB | ECMWF HUGO-m | ECMWF IB GLDAS | ECMWF HUGO-m GLDAS |
|---|---|---|---|---|---|---|
| CERGA | N005 | **9.078** | 9.593 | 9.737 | 9.653 | 9.797 |
| | N320 | 78.403 | **78.283** | 78.305 | 78.411 | 78.434 |
| Ste Croix-aux-Mines | N037 | 4.443 | 4.141 | 4.126 | 4.127 | **4.113** |
| | N120 | 4.033 | 3.990 | 3.975 | 3.970 | **3.959** |
| Infruts | N111 | **191.145** | 191.348 | 191.414 | 191.279 | 191.344 |
| | N324 | 106.529 | 106.464 | 106.391 | 106.462 | **106.389** |
| Titou | N011 | 51.716 | 51.433 | 51.435 | **51.432** | 51.433 |
| | N094 | **21.695** | 21.779 | 21.805 | 21.784 | 21.810 |
| Ploemeur | N080 | 512.174 | 511.471 | 509.775 | 511.376 | **509.680** |
| | N330 | 947.775 | 947.778 | **947.468** | 947.961 | 947.651 |

Table 3: RMS of tiltmeter residuals (in mas) after tidal analyses, and different global atmospheric, oceanic and hydrological loading corrections. The lowest value is shown in bold.